

Long-range transported dust enhances ice nucleating particles abundance and cloud formation in the North China Plain

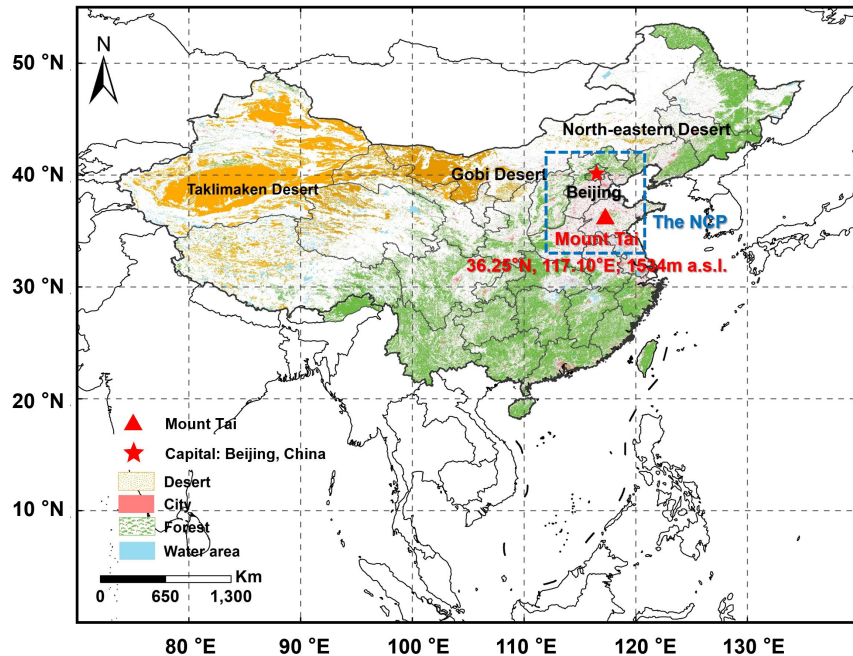
Yue Sun¹, Yujiao Zhu^{1*}, Hengde Liu², Lanxiadi Chen³, Hongyong Li¹, Yujian Bi², Di Wu², Xiangkun Yin²,
5 Can Cui¹, Ping Liu¹, Yu Yang¹, Jisheng Zhang¹, Yanqiu Nie¹, Lanxin Zhang¹, Jiangshan Mu¹, Yuhong Liu¹,
Zhaoxin Guo², Qinyi Li¹, Yuqiang Zhang¹, Xinfeng Wang¹, Mingjin Tang³, Wenxing Wang¹, and Likun
10 Xue¹

¹Environment Research Institute, Shandong University, Qingdao 266237, China

²Taishan National Reference Climatological Station, Tai'an 271000, China

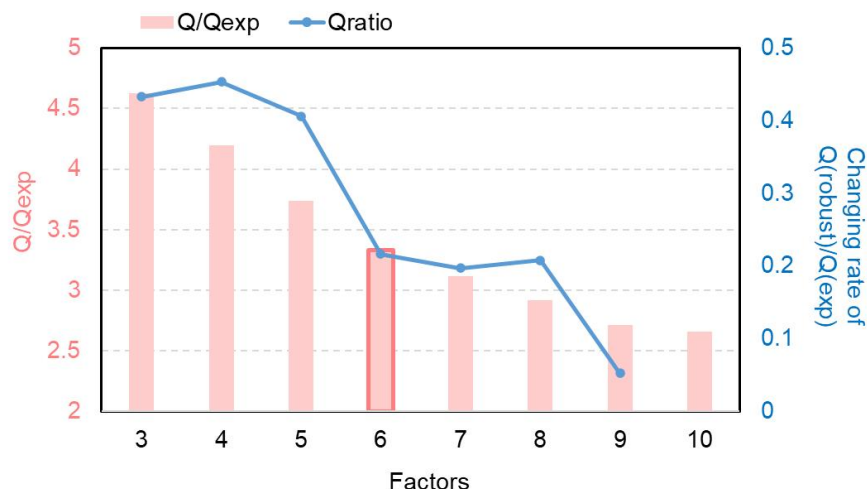
³State Key Laboratory of Advanced Environmental Technology, Guangzhou Institute of Geochemistry, Chinese Academy of Sciences, Guangzhou 510640, China

Correspondence to: Yujiao Zhu (zhuyujiao@sdu.edu.cn)



15

Figure S1. The geographical map showing the location of Mount Tai. This map is color-coded by land type (desert, city, forest, water area) and was downloaded from Resource and Environmental Science Data Platform (<https://www.resdc.cn/>, last access: 15 January, 2025). The blue dashed box represents the North China region, covering latitudes from 33°N to 42°N and longitudes from 112°E to 121°E.



20

Figure S2. Variation in the Q/Q_{expected} ratio with increasing numbers of PMF factors. The Q ratio represents the rate of change in Q between successive factor solutions and stabilizes when the number of factors reaches six

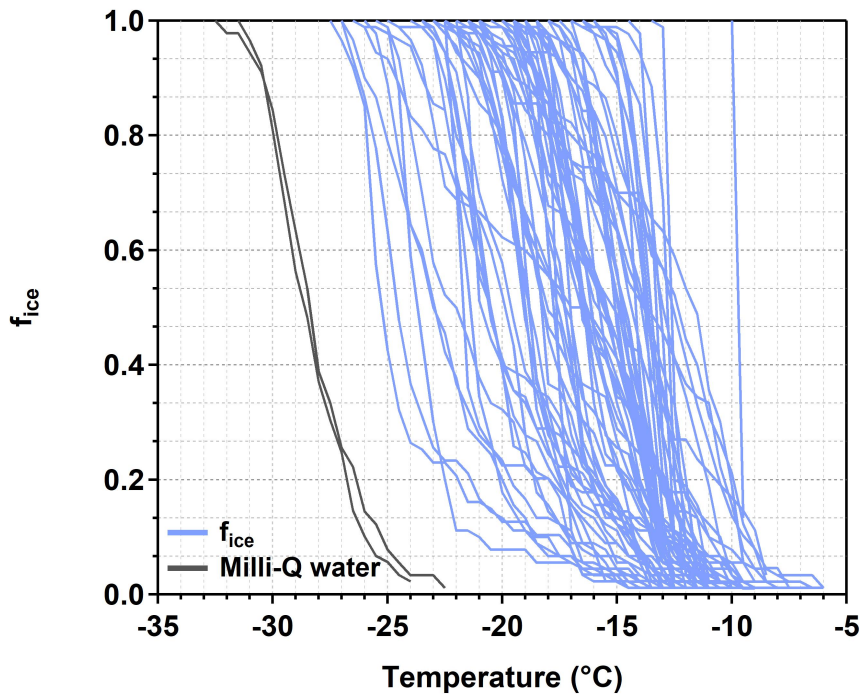


Figure S3. Frozen fractions of rainwater samples (f_{ice}) and Milli-Q water as a function of temperature.

25

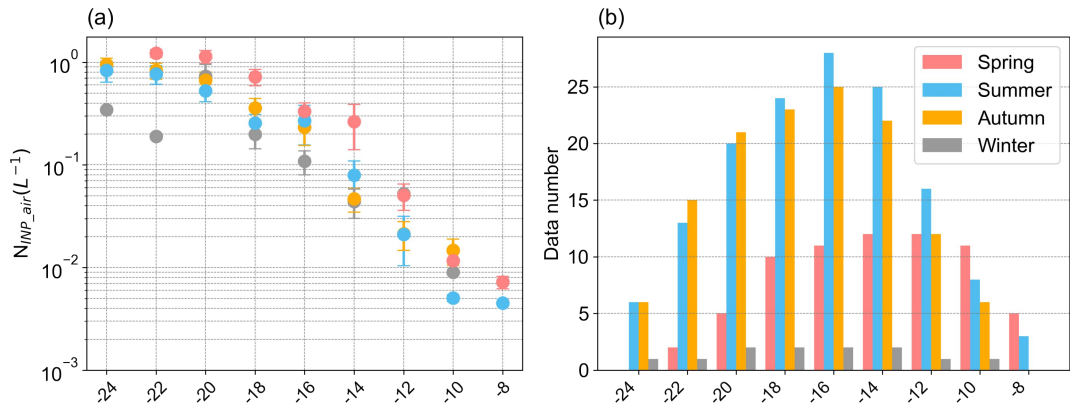
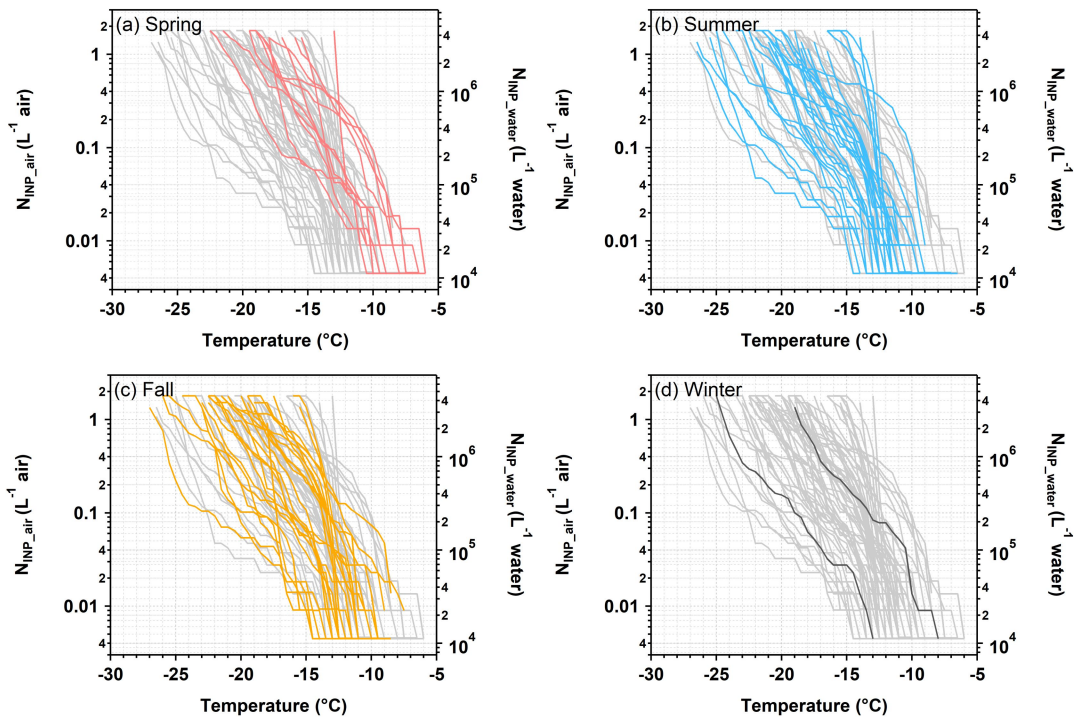


Figure S4. (a) Average N_{INP_air} and (b) the number of samples for different seasons as functions of temperature. The error bars represent the standard deviation.



30

Figure S5. N_{INP_air} for different seasons as a function of temperature. The light gray lines represent all rainwater samples.

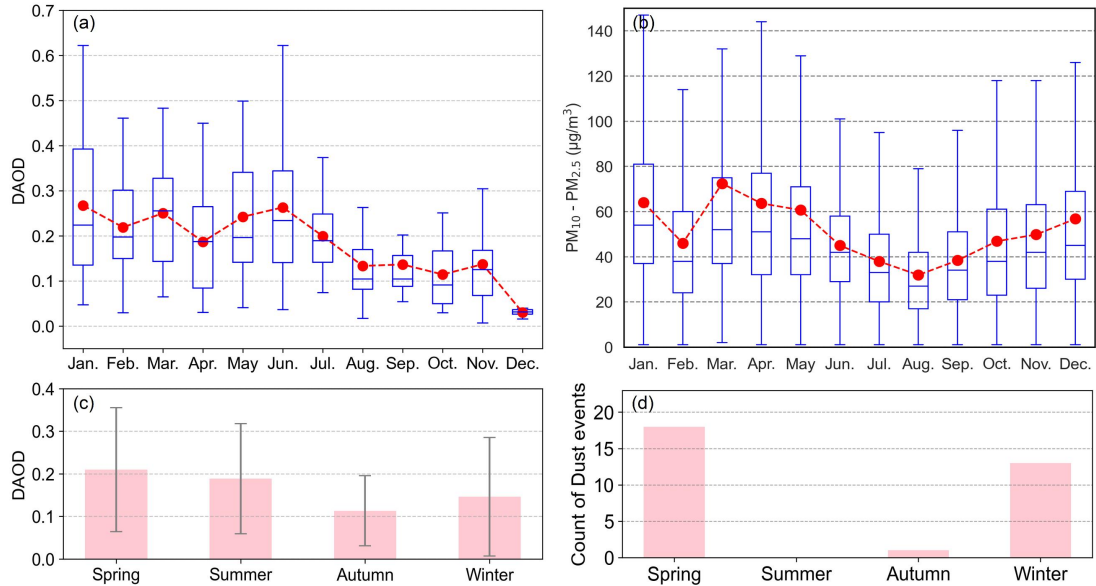


Figure S6. The monthly boxplots of (a) dust aerosol optical depth (DAOD) and (b) the mass concentration of the difference between PM_{10} and $PM_{2.5}$ ($PM_{10}-PM_{2.5}$) in 2021. The PM data at Tai'an city, located at the foothill of Mount Tai, were obtained from the China National Environmental Monitoring Center (CNEMC). The bottom and top edges of the box represent the 25th and 75th percentiles, respectively; the horizontal line within the box represents the median value; the whiskers represent the minimum and maximum values; and the red dots represent the mean concentrations. (c) Seasonal average DAOD with error bars representing the standard deviation. (d) The count of dust events identified using the criteria $PM_{10} > 150 \mu g/m^3$ and $PM_{2.5}/PM_{10} < 0.4$ over a 3-hour period, following the method of Wu et al. (2020).

35

40

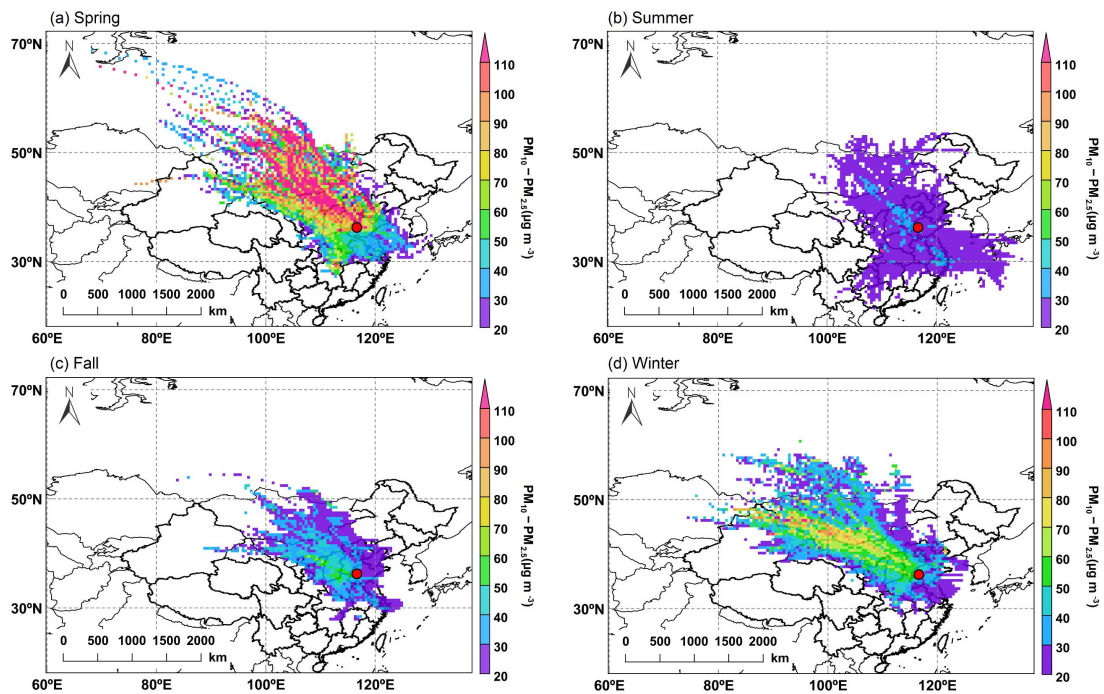


Figure S7. The 24-hour concentration-weighted trajectory (CWT) map of PM₁₀-PM_{2.5} for (a) Spring, (b) Summer, (c) Fall, and (d) Winter at Mount Tai (marked by the red circle) in 2021.

45

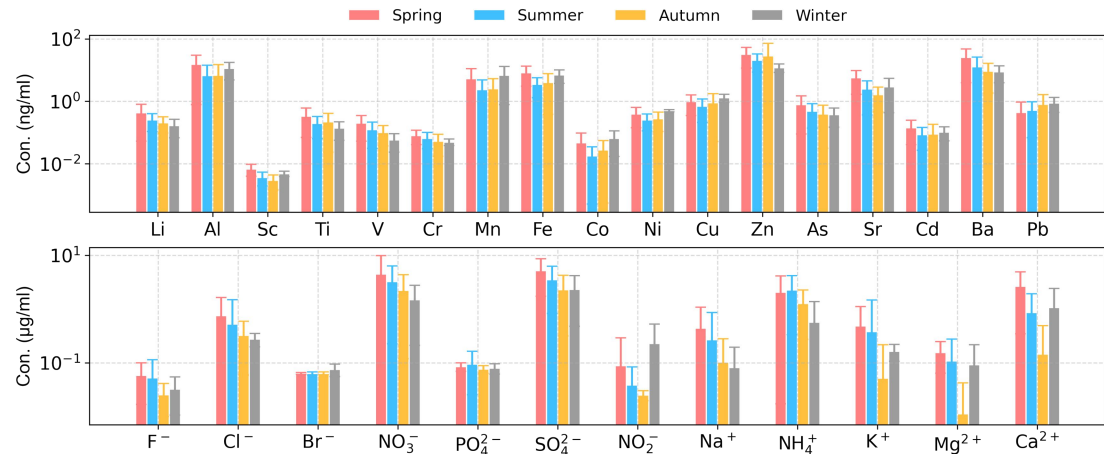
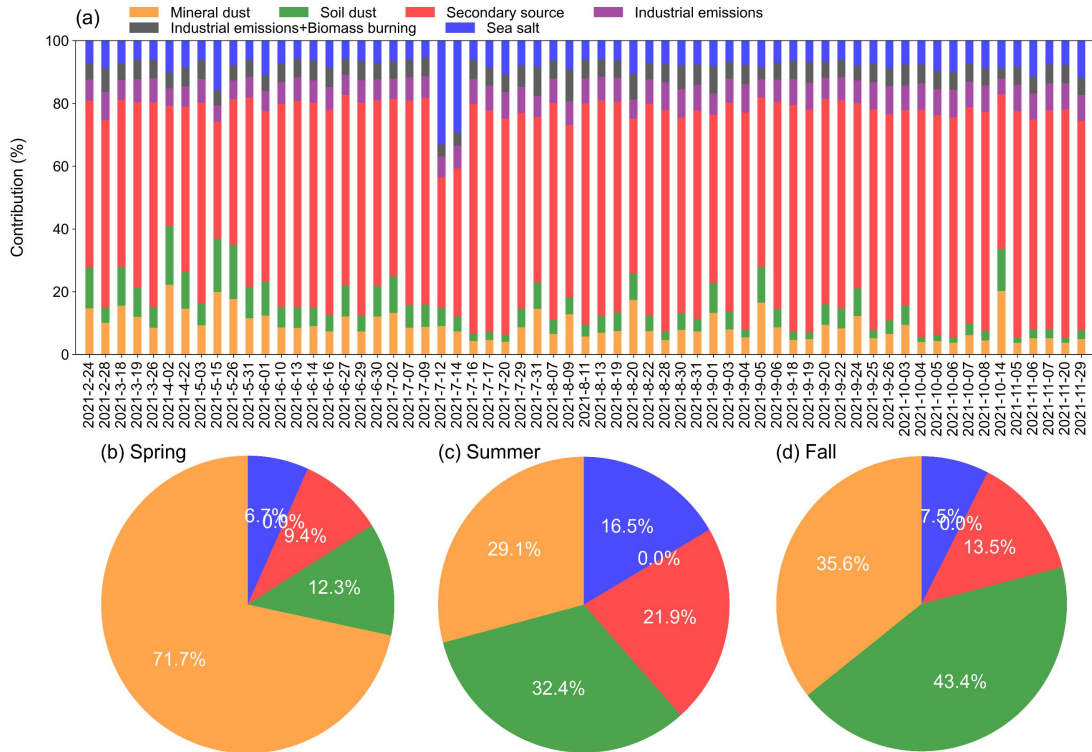


Figure S8. The average concentration of chemical components in different seasons. The error bars represent the standard deviation.



50

Figure S9. (a) The contribution of six identified factors during the sampling period. **(b-d)** Relative contributions of six sources to N_{INP_air} at -16°C during the sampling period in different seasons.

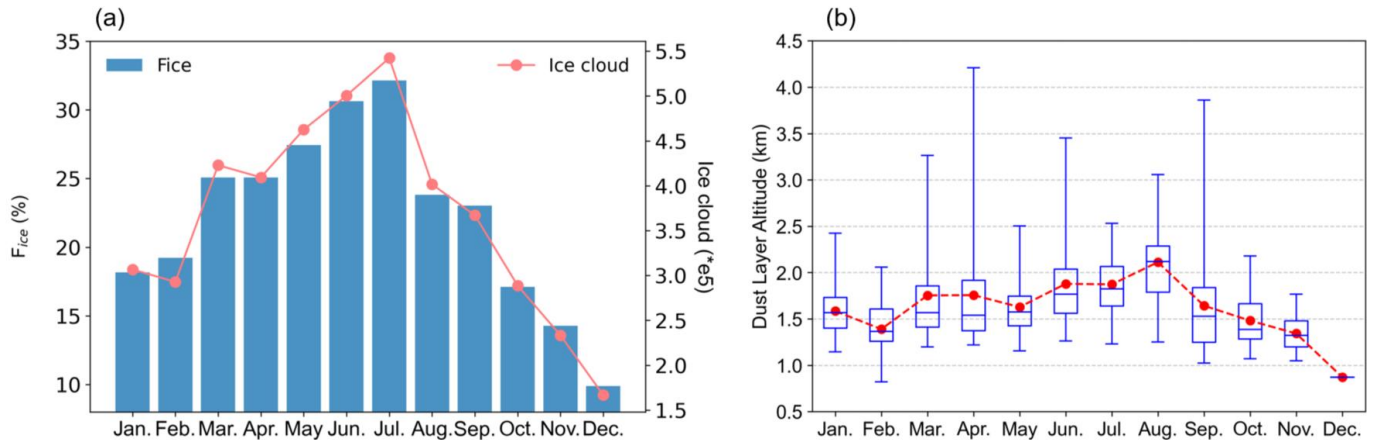


Figure S10. (a) The monthly fraction (F_{ice}) and count of ice clouds in 2021 over the NCP region (33°N - 42°N , 112°E - 121°E). **(b)** The monthly boxplot of average dust layer altitude in 2021. The bottom and top of the box represent the 25th and 75th percentiles, respectively, and the horizontal line inside the box represents the median value, the whiskers represent the minimum and maximum values, the red dots represent the mean values.

55

60

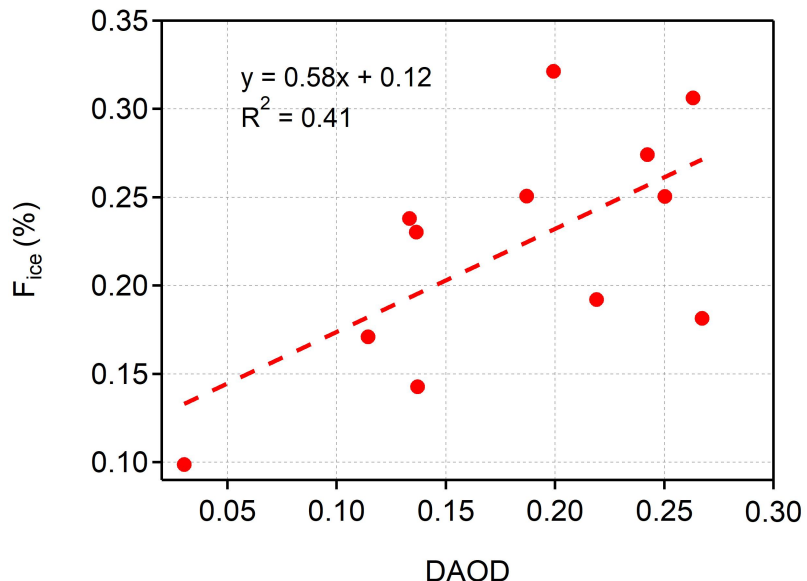


Figure S11. The relationship between DAOD and F_{ice} over the NCP in 2021.

References

65 Wu, C., Zhang, S., Wang, G. H., Lv, S. J., Li, D. P., Liu, L., Li, J. J., Liu, S. J., Du, W., Meng, J. J., Qiao, L. P., Zhou, M., Huang, C., and Wang, H. L.: Efficient heterogeneous formation of ammonium nitrate on the saline mineral particle surface in the atmosphere of East Asia during dust storm periods, Environ Sci Technol, 54, 15622-15630, <https://doi.org/10.1021/acs.est.0c04544>, 2020.